JETIR.ORG ISSN: 2349-5162 | ESTD Year : 2014 | Monthly Issue
JOURNAL OF EMERGING TECHNOLOGIES AND INNOVATIVE RESEARCH (JETIR)
An International Scholarly Open Access, Peer-reviewed, Refereed Journal

SYNTHESIS AND CHARACTERIZATION OF CeO_2–Zn NANOPARTICLES FOR PHOTOCATALYTIC APPLICATIONS

[1] Masku Vidyani, [2] Dr. P. Ranjith Reddy
[1] Project Student, [2] Assistant Professor
[1]Department of Physics,
[1]JNTUH University College of Engineering, Science and Technology, Hyderabad, Telangana, India

Abstract
This study reports the synthesis of CeO_2–Zn nanoparticles using the sol–gel method and their evaluation for photocatalytic activity. Structural[1], morphological, and optical properties were analyzed using XRD, FTIR[2], and UV–Vis spectroscopy[3]. The photocatalytic efficiency was assessed using methyl orange (MO) dye degradation under sunlight irradiation. Zn doping improved charge separation and visible-light absorption, enhancing degradation efficiency compared to pure CeO_2. The results highlight the potential of CeO_2–Zn nanocomposites for environmental remediation.

Keywords: CeO_2, Zn doping, Nanoparticles, Photocatalysis, Sol–gel.

I. INTRODUCTION

Water pollution from industrial dyes is a major concern, particularly in developing countries[4] where untreated effluents often enter natural water bodies. Synthetic dyes such as methyl orange, widely used in textiles and plastics, are non-biodegradable, carcinogenic, and resistant to conventional treatments[5]. Semiconductor photocatalysis has emerged as a sustainable approach for degrading such pollutants. Among metal oxides, CeO_2 has gained attention for its redox properties, oxygen storage capacity, and chemical stability[6]. However, its wide band gap (~3.2 eV) and rapid electron–hole recombination restrict efficiency. Metal ion doping, especially with Zn^{2+}, reduces the band gap, enhances charge separation, and generates oxygen vacancies, thereby improving photocatalytic performance [7].

In this study, CeO_2 and Zn-doped CeO_2 nanoparticles were synthesized via a low-cost sol–gel route. Pure CeO_2 was prepared using cerium nitrate as a precursor, while CeO_2–Zn nanocomposites were obtained by introducing zinc nitrate into the same sol–gel process. The structural, morphological, and optical properties of both samples were characterized, and their photocatalytic activity was evaluated through methyl orange degradation under sunlight [8]. The effect of Zn doping on degradation efficiency and kinetics was systematically investigated, highlighting the potential of CeO_2–Zn nanocomposites for environmental remediation.

II. EXPERIMENTAL SETUP AND METHODOLOGY:

$Ce(NO_3)_3 \cdot 6H_2O$ and $Zn(NO_3)_2 \cdot 6H_2O$ were used as precursors[9], with citric acid as a chelating agent and ammonia for pH adjustment[10]. The sol–gel method involved hydrolysis[11], condensation[12], gelation[13], drying at 100–120 °C, and calcination at 500–550 °C to obtain nanopowders. Pure CeO_2 nanoparticles were synthesized using only cerium nitrate, while CeO_2–Zn nanocomposites were prepared by adding zinc nitrate to the same process.

Characterization was carried out using XRD (phase structure and crystallite size), FTIR (metal–oxygen bonding and surface groups), and UV–Vis spectroscopy (optical absorption). Photocatalytic activity was tested by degrading aqueous methyl orange solutions under UV–visible irradiation, comparing the performance of pure CeO_2 and Zn-doped CeO_2 samples.

III. RESULTS AND DISCUSSIONS:

3.1. XRD Analysis:

The XRD patterns of CeO_2 and Zn–CeO_2 nanoparticles (Figure 1) exhibit distinct reflections at (111), (200), (220), (311), (222), and (400), characteristic of cubic fluorite[14] CeO_2 (JCPDS 34-0394)[15] , No secondary ZnO or Ce_2O_3 phases were detected, confirming successful incorporation of Zn into the CeO_2 lattice[16].

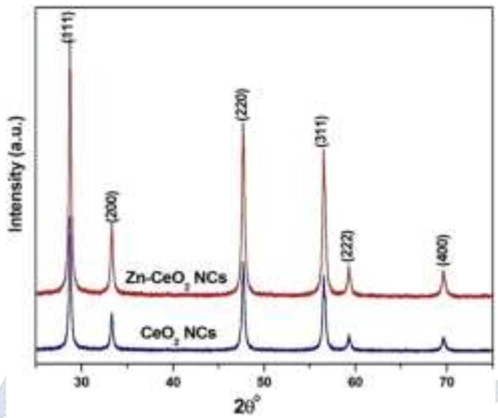

Figure.1 XRD patterns of CeO_2 and Zn–CeO_2 nanoparticles

Zn doping caused slight peak broadening and minor shifts, indicating reduced crystallite size, lattice distortion, and oxygen vacancy formation. Crystallite sizes, estimated using the Scherrer equation[17], were in the nanometer range. These structural modifications are expected to enhance photocatalytic performance by improving charge separation and providing more active surface sites.

3.2. FTIR Analysis:

The FTIR spectra of CeO_2 and Zn–CeO_2 nanoparticles (Figure 2) display strong absorption bands around 500–600 cm^{-1}, attributed to Ce–O stretching vibrations, confirming the fluorite structure. In the Zn–CeO_2 spectrum, these peaks broaden and shift slightly, indicating Zn incorporation and lattice distortion.

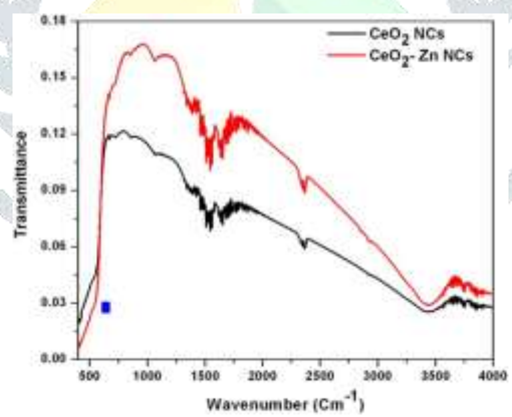

Figure.2 FTIR spectra of CeO_2 and Zn–CeO_2 nanoparticles

Broad bands near 3400 cm^{-1} and around 1400–1600 cm^{-1} correspond to O–H stretching and bending modes, suggesting surface hydroxyl groups[18] and adsorbed water. Their higher intensity in Zn–CeO_2 indicates enhanced hydroxylation, which facilitates the formation of reactive hydroxyl radicals during photocatalysis. Weak features between 1100–1400 cm^{-1} are associated with residual carbonates from the sol–gel process. Overall, FTIR confirms the structural integrity of CeO_2 and highlights surface modifications induced by Zn doping that contribute to improved photocatalytic activity.

3.3. UV–Vis Analysis:

UV–Vis absorption spectra (figure 3) revealed that pure CeO_2 exhibits strong absorption in the UV region, consistent with its wide band gap (~3.2 eV). Upon Zn doping, the absorption edge shifted slightly toward the visible region, indicating band gap narrowing.

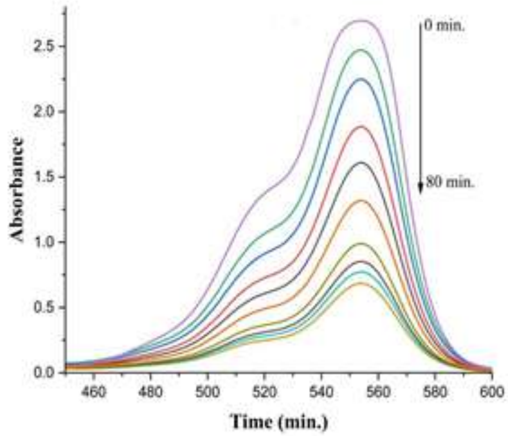

Figure.3 UV–Vis absorption spectra

The optical band gap (E_g) was estimated using Tauc's relation $(\alpha h\nu)^2 \propto (h\nu - E_g)$, where extrapolation of the linear region of the plot gave smaller values for Zn–CeO_2 compared to pure CeO_2. This reduction in band gap enhances visible-light absorption and contributes to improved photocatalytic activity.

IV. CONCLUSION

CeO_2 and Zn–doped CeO_2 nanoparticles were successfully synthesized using the sol–gel method. XRD confirmed the cubic fluorite structure with reduced crystallite size and lattice distortion upon Zn incorporation. FTIR spectra verified Ce–O bonding and revealed enhanced surface hydroxylation in Zn–CeO_2, favorable for photocatalysis. UV–Vis analysis showed a redshift in the absorption edge and band gap narrowing, improving visible-light response. These structural and optical modifications collectively enhance the photocatalytic efficiency of Zn–doped CeO_2, demonstrating its potential for wastewater treatment and environmental remediation.

REFERENCES:

[1] Patterson, A. L. (1939). The Scherrer formula for X-ray particle size determination. Physical Review, 56(10), 978–982.

[2] Smith, A. L. (1979). Applied Infrared Spectroscopy. Wiley-Interscience, New York.

[3] Tauc, [4]Robinson, T., McMullan, G., Marchant, R., & Nigam, P. (2001). Remediation of dyes in textile effluent: a critical review on current treatment technologies with a proposed alternative. Bioresource Technology, 77(3), 247–255.

[4] Robinson, T., McMullan, G., Marchant, R., & Nigam, P. (2001). Remediation of dyes in textile effluent: a critical review on current treatment technologies with a proposed alternative. Bioresource Technology, 77(3), 247–255.

[5] Forgacs, E., Cserháti, T., & Oros, G. (2004). Removal of synthetic dyes from wastewaters: a review. Environment International, 30(7), 953–971.

[6] Tuller, H. L. (2016). Defect chemistry in oxides. Annual Review of Materials Research, 46, 465–489.

[7] Wang, Z., Yang, J., & Li, C. (2006). Band-gap engineering of CeO_2 nanoparticles by transition metal doping. Applied Physics Letters, 89(16), 163123.

[8] Sun, C., Li, H., & Chen, L. (2012). Nanostructured ceria-based materials: synthesis, properties, and applications. Energy & Environmental Science, 5(9), 8475–8505.

[9] Patel, M., & Patel, K. (2019). Synthesis and characterization of Zn-doped CeO_2 nanoparticles for photocatalytic activity. Materials Today: Proceedings, 18, 1862–1867.

[10] Sanchez, C., Julián, B., Belleville, P., & Popall, M. (2005). Applications of hybrid organic–inorganic nanocomposites. Journal of Materials Chemistry, 15(35–36), 3559–3592.

[11] Klein, L. C. (1990). Sol-gel processing of ceramics and glasses. Materials Research Society Bulletin, 15(6), 34–39.

[12] Innocenzi, P. (1999). Infrared spectroscopy of sol–gel derived silica-based films: A spectra–structure correlation. Journal of Non-Crystalline Solids, 316(2–3), 309–319.

[13] Livage, J., Henry, M., & Sanchez, C. (1988). Sol–gel chemistry of transition metal oxides. Progress in Solid State Chemistry, 18(4), 259–341.

[14] Burroughs, P., Hamnett, A., Orchard, A. F., & Thornton, G. (1976). Satellite structure in the X-ray photoelectron spectra of some binary and mixed oxides of lanthanum and cerium. Journal of the Chemical Society, Dalton Transactions, (17), 1686–1698.

[15] Joint Committee on Powder Diffraction Standards (JCPDS). (1998). Card No. 34-0394, International Centre for Diffraction Data, Pennsylvania, USA.

[16] Babu, B., & Reddy, M. P. (2016). Structural and optical properties of Zn-doped CeO_2 nanoparticles. Material Science.

[17] Patterson, A. L. (1939). The Scherrer formula for X-ray particle size determination. Physical Review.

[18] Bellamy, L. J. (1975). The Infrared Spectra of Complex Molecules. Chapman and Hall, London.eview, 56(10), 978–982.ials Science in Semiconductor Processing, 41, 491–497.